Predicting the stochastic guiding of kinesin-driven microtubules in microfabricated tracks: A statistical-mechanics-based modeling approach

Chih-Tin Lin
Department of Electrical Engineering, National Taiwan University, Taipei 106, Taiwan

Edgar Meyhofer*,† and Katsuo Kurabayashi*,‡
Department of Mechanical Engineering, University of Michigan, Ann Arbor, Michigan 48109, USA
(Received 17 August 2009; revised manuscript received 28 November 2009; published 29 January 2010)

Directional control of microtubule shuttles via microfabricated tracks is key to the development of controlled nanoscale mass transport by kinesin motor molecules. Here we develop and test a model to quantitatively predict the stochastic behavior of microtubule guiding when they mechanically collide with the sidewalls of lithographically patterned tracks. By taking into account appropriate probability distributions of microscopic states of the microtubule system, the model allows us to theoretically analyze the roles of collision conditions and kinesin surface densities in determining how the motion of microtubule shuttles is controlled. In addition, we experimentally observe the statistics of microtubule collision events and compare our theoretical prediction with experimental data to validate our model. The model will direct the design of future hybrid nanotechnology devices that integrate nanoscale transport systems powered by kinesin-driven molecular shuttles.

DOI: 10.1103/PhysRevE.81.011919 PACS number(s): 87.16.Ka, 81.16.Rf, 87.85.−d, 89.20.−a

I. INTRODUCTION

Nanometer-scale mass transport mechanisms driven by molecular machinery in living cells are widely expected to find practical applications in bionanotechnology. Toward this goal, recent studies have pioneered first hybrid nanodevices that integrate cytoskeletal protein filaments (e.g., microtubules) moving on a surface coated with motor proteins (e.g., kinesin) for molecular sorting [1,2], biosensing [3,4], fluidic pumping [5], micromechanical powering [6], and molecular assembly [7]. Loaded with other biomolecules or engineered microstructures, kinesin-driven microtubules serve as "molecular shuttles" in these devices, and transport the various cargos by efficiently converting chemical energy stored in ATP into mechanical work [8]. Microtubule guiding via microfabricated channels or tracks has been widely used as a promising method to precisely control the direction of motion and final destination of the molecular shuttles [6,9,10]. This method is based on the mechanical interactions of kinesin-driven microtubules with the sidewalls of tracks. Since the microscopic collision events are inherently stochastic in nature, only a fraction of the microtubules are successfully redirected while others detach from the kinesin-coated surface and diffuse into solution or are steered into the wrong direction. The goal of this work is to develop the theoretical framework for enabling a systematic understanding of the physical and biophysical mechanisms of this collision process and ultimately design a highly efficient microtubule guiding mechanism.

In this paper, we propose a statistical-mechanics model to analyze the stochastic phenomena associated with the microtubule guiding process. While past theoretical simulations using computational algorithms such as Monte Carlo methods [11] have provided first insights (or made first attempts at characterizing this guiding process), there exists a fundamental knowledge gap in our understanding of the mechanics and mechanistic principles of microtubule-track interactions that quantitatively control the guiding of microtubules [12]. Our model allows us to quantitatively analyze these principles.

In Sec. II, we describe our model for a kinesin-driven microtubule upon its collision with a lithographically patterned microchannel sidewall and derive a formula for the probability of successful guiding events through accounting for a canonical ensemble of microstates of the microtubule system characterized by its free end bending configurations. In Sec. III, we carry out microtubule guiding assays using a microfabricated track on a kinesin-coated glass substrate and quantitatively measure the probability of successful microtubule redirection events. In Sec. IV, a theoretical prediction derived from the model in Sec. II is compared with the experimental data obtained in Sec. III to show the validity of our theoretical approach. We conclude our study in Sec. V with a discussion of the results and their physical implications.

II. STATISTICAL MODEL

A. Microtubule collision

The microtubule guiding process is illustrated in Fig. 1(a), where a kinesin-driven microtubule collides with the track sidewall at the angle θ (the approach angle). Based on our previous work [6], it is well established that the vertical surfaces of our microfabricated tracks (see below) adsorb no functional kinesin motors and consequently yields no microtubule motility on them. Therefore, we assume that the movement of the microtubule is driven entirely by kinesin molecules located on the bottom glass surface of the channel.

*Corresponding authors.
†meyhofer@umich.edu
‡katsuo@umich.edu

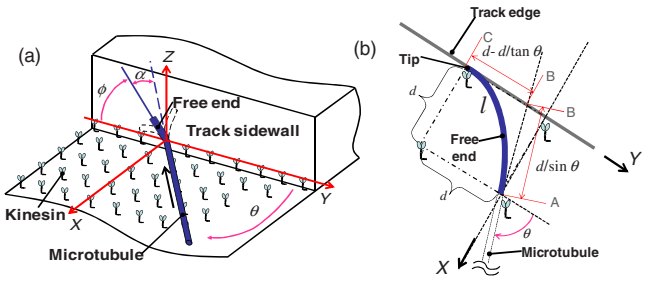

FIG. 1. (Color online) Illustration of microtubule guiding by a microfabricated track. (a) Schematic of a kinesin-driven microtubule colliding with the track sidewall. The drawing represents an (instantaneous) snapshot during the mechanical intercounter between microtubule and the track sidewall. The microtubule approaches the wall at an angle θ $(0<\theta<90°)$ and experiences elastic bending of its free end that is detached from the kinesin-coated surface (the X-Y plane). The free end may also be bent up at an angle ϕ on the track sidewall plane (the Y-Z plane), where its length is given by l (b) Detailed geometry of the tip of the microtubule free end that is recaptured by the nearest kinesin on the channel surface (the X-Y plane) due to diffusion. The curved line representing the free end is approximated with the two straight lines AB and BC so that $l \approx AB+BC=d/\sin\theta+[d-d/\tan\theta]$.

Upon mechanical collision of the thermally fluctuating tip of the microtubule with the sidewall, the unattached front segment of the microtubule (the portion of the leading end of the microtubule not interacting with motors) is bent and the tip is sliding along the sidewall driven by the continuous movement of the microtubule. From our experimental observations, we find that the microtubule continues to glide toward the wall with its free end pointing into the wall and experiences buckling at the channel edge very infrequently at a probability less than 1%. This suggests that the friction between the tip and the channel sidewall is small. As a result, our model only accounts for a microtubule system *after* its tip is bent on the sidewall, neglecting rare buckling events.

Since the interactions of sliding microtubules with the sidewall are stochastic in nature, the resulting motion of the microtubule tip along the sidewall will proceed into variable directions with respect to the nominal direction defined by the angle ϕ (the free end angle) from the horizontal direction (i.e., $-Y$ direction) and may lead to the release of the microtubule from the kinesin-coated surface. We expect the probability of the release in microtubules guiding also to depend on the approach angle, as the magnitude of force components acting on the microtubule tips is angle dependent. We set the surface distribution of kinesin molecules to be uniform where the spacing between kinesin motors is distance d. As a first-order approximation it is assumed that the friction on the track sidewall is negligible, having no effect on the free end fluctuations. The movement of the free end on the track sidewall plane (the Y-Z plane) may allow the nearest kinesin on the channel surface to recapture the leading tip of the microtubule such that its pathway is directed along the track edge [Fig. 1(b)]. Here, the microtubule continues to be transported along the track, thus making the redirection process successful. Alternatively, thermal fluctuations may direct the tip of the microtubule to interact with the track's sidewall in such a way that the microtubule is pushed upward on the Y-Z plane. Such upward deflection is then likely to continue until the whole microtubule is fully detached and eventually diffuses away from the kinesin-coated surface.

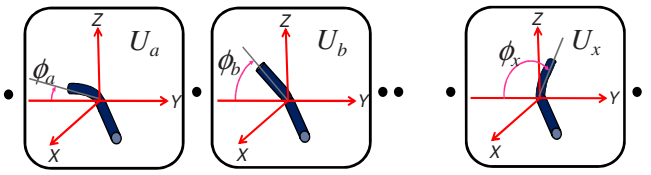

FIG. 2. (Color online) Canonical ensemble of microstates of a microtubule characterized by its free end configuration. The microstate energy U takes continuum values determined by the tip angle ϕ. The partition function of such a classical system, as opposed to a quantum mechanical system, is given by integrating the Boltzmann factor with respect to ϕ as $Z=\int_0^{\pi}\exp(-\frac{U_\theta^{(d)}(\phi')}{k_BT})d\phi'$.

B. Microstates of microtubule system

From our experimental observation, the length of the microtubule is typically on the order of 10 μm, much smaller than its persistence length of several millimeters [13–15]. This allows us to treat the microtubule as an elastic cylindrical rod with mechanical flexibility according to the wormlike chain (WLC) model in polymer physics [16]. Here, the bending energy stored in the microtubule is given by $U=\frac{EI}{2l}\alpha^2$ [15], where α is the bending angle of the microtubule free end, $l \approx d+d(1-\cos\theta)/\sin\theta$ is the length of the microtubule free end [Fig. 1(b)], E is the Young's modulus of the microtubule, and I is the second moment of inertia of the microtubule, and EI, the product of E and I, represents the flexural rigidity of the microtubule. Here, the tip length l is taken as the length required for the tip to be recaptured by the nearest available kinesin on the X-Y plane due to thermal fluctuations. In the XYZ coordinates, the unit vector parallel to the microtubule approach direction and the one parallel to the microtubule free end direction are given by $\mathbf{u}_\theta=-\sin\theta\mathbf{i}-\cos\theta\mathbf{j}$ and $\mathbf{u}_\phi=-\cos\phi\mathbf{j}+\sin\phi\mathbf{k}$, respectively. Since α is the angle formed by these two directions, the bending angle of the microtubule is readily determined from the relationship $\mathbf{u}_\theta\cdot\mathbf{u}_\phi=\cos\alpha=\cos\theta\cos\phi$. Then, the bending energy U is given in terms of the kinesin interspace distance d and the tip angle ϕ at a given value of θ by

$$U = U_\theta^{(d)}(\phi) = \frac{EI}{2d[1+(1-\cos\theta)/\sin\theta]}[\cos^{-1}(\cos\theta\cos\phi)]^2. \quad (1)$$

For our model, we consider a canonical ensemble of microstates of the microtubule system characterized by free end bending configurations defined by ϕ, for which quasiequilibrium conditions are assumed [Fig. 2]. We approximate time serial changes in the collision-induced microtubule free end bending to be a series of processes in thermal equilibrium. The probability of occupancy of the specific microstate at ϕ is given by the Boltzmann factor,

$$p_\theta^{(d)}(\phi) = \exp\left(-\frac{U_\theta^{(d)}(\phi)}{k_B T}\right) \Bigg/ \int_0^\pi \exp\left(-\frac{U_\theta^{(d)}(\phi')}{k_B T}\right) d\phi', \tag{2}$$

where $k_B = 1.38 \times 10^{-23}$ JK^{-1} is the Boltzmann constant and T is the temperature.

C. Critical free end angle

Now, we consider the diffusion process of the thermally fluctuating microtubule free end for its tip to be caught by the next available kinesin along the track edge. The passage time needed for the tip to find the next available kinesin is derived from the knowledge of the trajectory between the initial state with the free end bent on the sidewall and the final state with the end bound with the kinesin at $\phi=0$, and from the activation energy along the passage, ΔU_a. For simplicity, we approximate ΔU_a with the bending energy difference between the initial and final states as $\Delta U_a \approx U_\theta^{(d)}(\phi) - U_\theta^{(d)}(0)$ following the formulation by Howard [17]. Assuming $\Delta U_a \gg k_B T$, the first passage time is given by

$$t_k = \tau \sqrt{\frac{\pi}{4}} \sqrt{\frac{k_B T}{\Delta U_a}} \exp\left(\frac{\Delta U_a}{k_B T}\right), \tag{3}$$

where τ is the relaxation time that can be estimated as [13]

$$\tau \cong \frac{c_\perp}{EI}\left(\frac{l}{(n+1/2)\pi}\right)^4. \tag{4}$$

In Eq. (4), n represents the nth vibration mode of the microtubule tip, which is chosen to be $n=1$ assuming only the first mode is the primary contributor to the tip vibration, and $c_\perp$ is the perpendicular drag coefficient per unit length,

$$c_\perp = \frac{4\pi\eta}{\cosh^{-1}(1 + b/r)}, \tag{5}$$

where $\eta = 1 \times 10^{-3}$ kg/m s is the viscosity of water at room temperature, $b = 11$ nm is the height of the microtubule cylinder axis, and $r = 15$ nm is the microtubule hydrodynamic radius [18]. For a microtubule guiding or redirection process to be successful, the first passage time t_k needs to be shorter than the microtubule drift time t_d, which is estimated by the time in which the microtubule travels a distance equal to its free end l. This condition calls for

$$t_k \leq t_d = l/v_m, \tag{6}$$

where v_m is the travel speed of the microtubule. From Eq. (6), we can calculate the critical free end angle β, which is the upper bound for the value of ϕ leading to a successful guiding event, i.e., when the free end angle ϕ exceeds the critical angle β, the microtubule diffuses away from the kinesin-coated surface [Fig. 3].

With the critical angle β determined for a given value of θ as $\beta = \beta(\theta)$, the probability of success of the microtubule guiding process $P^{(d)}(\theta)$ is given by integrating the occupancy probabilities of these contributing microstates,

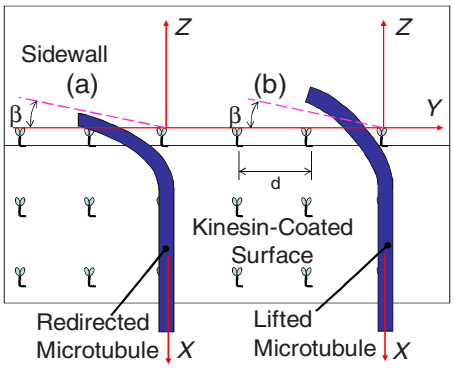

FIG. 3. (Color online) Configurations of the microtubule free end bending (a) succeeding and (b) failing the guiding process for the specific approach angle $\theta=90°$. The free end angle is $\phi<\beta$ in (a), where the tip will subsequently be recaptured by the nearest kinesin along the track edge. In contrast, the free end angle is $\phi>\beta$ in (b), where the energy required for the tip to be recaptured becomes so large that it will remain detached from the kinesin-coated surface.

$$P^{(d)}(\theta) = \int_0^{\beta(\theta)} p_\theta^{(d)}(\phi) d\phi, \tag{7}$$

where we take into account that microstates at $0<\phi<\beta(\theta)$ only contribute to successful microtubule guiding events.

III. EXPERIMENT

Microtubule guiding assays are performed on test chips with a microfabricated track to obtain data that we can compare with our model prediction. The track is constructed by patterning a 1.5-μm-thick layer of amorphous fluoropolymer, CYTOP (Asahi Glass, Co., Tokyo, Japan) deposited on a cover glass substrate. We perform the track fabrication following the standard photoresist lithography coupled with reactive ion etch using a SF_6 gas. Prior to each assay, the entire chip surface is pretreated with aqueous solution of casein and then washed with BRB80 buffer.

For our experiments, we use a bacterially expressed kinesin motor, NKHK560cys. This motor consists of the head and neck domain of *Neurospara crassa* kinesin (amino acids 1–433) and stalk of *Homo sapiens* kinesin (residues 430 to 560) and a reactive cysteine at C-terminal end. Tetramethyl rhodamine (TMR)-labeled microtubules are polymerized using a protocol described in [6]. Our experiments employ a protein loading procedure identical to that for standard kinesin gliding assays: chambers are loaded with kinesin (47 μg/ml casein and 1.6 μM kinesin in BRB80 buffer) and incubated for 5 min. Subsequently, microtubules in a BRB80 buffer containing 1 mM ATP and an oxygen scavenger system (4 μg/ml microtubules, 2 mM $MgCl_2$, 10 mM glucose, 100 μg/ml glucose oxidase, 80 μg/ml catalase, 10mM DTT, and 47 μg/ml casein) are loaded.

We observe samples with an inverted fluorescence microscope (Zeiss Axiovert 200, 40×/1.3 NA Plan Neofluar objective), and images are recorded with a digital charge-coupled device camera (Orca II, Hamamatsu, Japan). From the re-

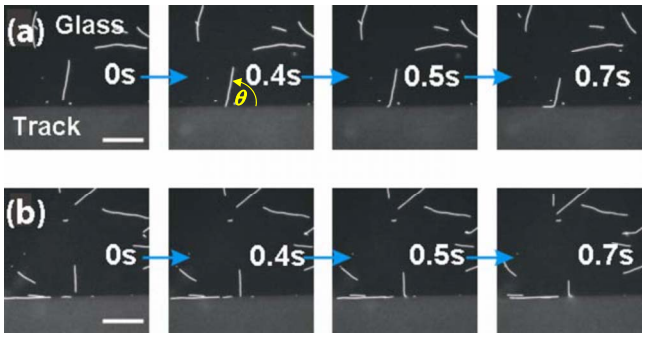

FIG. 4. (Color online) Image sequence of the microtubule guiding assays. (a) A microtubule approaching at an angle of $\theta=82°$ is guided along the CYTOP track after colliding with the sidewall. (b) A microtubule approaching at a right angle is lifted off from the kinesin-coated glass surface starting with its leading end and eventually disappears from the field of view. Scale bar is 10 μm.

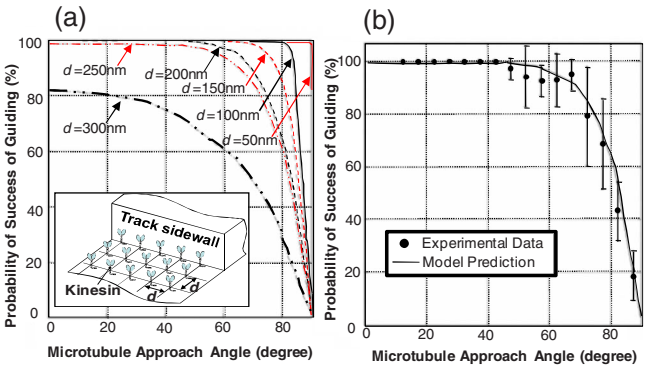

FIG. 5. (Color online) (a) Probability of success of the microtubule guiding process with respect to the microtubule approach angle θ, predicted by the statistical mechanical model for various kinesin interspace distances ($d=50-300$ nm). It is predicted that the success rate becomes nearly 100% at any approach angle for a kinesin-to-kinesin distance less than 50nm. (b) Results of the guiding assays using NKHK560cys kinesin-driven microtubules, compared to a model prediction curve assuming $EI=8\times10^{-24}$ Nm^2 and $d=200$ nm. The error bar of each data point represents the standard deviation for the statistical distribution of microtubule guiding events observed with sample sizes ranging from 160–320.

corded images, we track the motion trajectories and approach angles of individual microtubules. We consider the guiding process as successful when a microtubule aligns itself with the track and continues to travel for at least 3 μm past the collision site [Fig. 4(a)]. In contrast, the process is scored as a failed redirection event if the microtubule fully detaches from the surface after the collision. The full detachment of the microtubule is verified when we observe the tip starting to look blurred, eventually leading to the entire fluorescent image of the microtubule disappearing from the field of view at focus [Fig. 4(b)]. In our measurements, the probability of success in the guiding process is defined as the ratio of the number of successful guiding events to the total number of collision events with respect to each incident angle.

IV. MODEL VALIDATION

Equation (7) indicates that the microtubule guiding process is affected by both the approach angle θ and the kinesin interspace distance d, correlating with the kinesin surface density given by $\sigma=1/d^2$. In Fig. 5(a), we show calculated probabilities of success with respect to the approach angle θ varying between 0 and 90° for various values of d. Our model predicts that larger kinesin surface density (100 $\sim$400 μm^{-2}) yields a success rate higher than 80% even at steep approach angles $>80°$, which cause large elastic bending energy (typically >1000 k_BT at room temperature) to be stored in the microtubule. Figure 5(b) plots both experimental data and a theoretical curve. The theoretical curve matches the data within the standard deviation. To analyze our experimental data, we assume that the microtubule flexural rigidity is $EI=8\times10^{-24}$ Nm^2 from data in literature [14] and that the kinesin surface density is $\sigma=25$ μm^{-2}, which translates into the kinesin interspace distance $d=200$ nm. This surface density is comparable to that measured for a casein-coated glass surface by Katira *et al.* [19] ($\sigma=1-30$ μm^2) prepared under a surface treatment similar to that of our protocol. It follows that our model yields a theoretical prediction in good agreement with measurements assuming experimentally viable values for these parameters.

Typical values of the microtubule flexural rigidity reported in previous studies [13,14,20–22] lie in the range of $0.8-4\times10^{-23}$ Nm^2. The particular value of EI (0.8×10^{-23} Nm^2) employed in our model calculation above is consistent with recent work of [22] that incorporates findings on the length dependence and anisotropic behavior of microtubules and is appropriate for microtubules in the length range as studied here. To evaluate the sensitivity of the flexural rigidity EI on the expected kinesin surface density σ extracted from the theoretical curve fitting, we find that, for example, doubling of the value of the microtubule's flexural rigidity EI from 0.8×10^{-23} to 1.6×10^{-23} Nm^2 results in a change in the estimated value of d from 200 to 245 nm, which translates into a decrease in σ by a factor of 1.5. A larger flexural rigidity of the microtubule yields a higher frequency of the thermal fluctuation of its free end as indicated by the smaller value of τ derived in Eq. (4), which facilitates the recapturing events. The more frequent recapturing events contribute to the fact that the value of d extracted from the curve fitting also becomes larger at the larger value of EI, leading to the smaller value of σ.

V. CONCLUSIONS

In this paper, we have developed a statistical-mechanics model to analyze the stochastic nature of microtubule guiding by a lithographically patterned track. By experimentally characterizing the collision behavior of microtubules at a microfabricated track sidewall of nonmotile amorphous fluoropolymer, we have shown that the model can accurately predict experimental results. The model provides insight into the influence of two key factors: (1) the microtubule approach angle and (2) the kinesin surface density, on the success rate of the microtubule guiding process. Once a value of the flexural rigidity of microtubules can be precisely identi-

fied from independent experiment under relevant conditions, our theoretical approach will make it possible to estimate the surface density of kinesin from microtubule guiding assay data. Our theoretical finding suggests that the microtubule guiding process can be significantly improved by increasing the kinesin surface density. A physics-based understanding of effects of track geometries and topographies on microtubule guiding is crucial for mechanistic design of molecular shuttle-based hybrid nanodevices, eliminating iterative trial-and-error processes. We believe that the model developed here will be critical to guide the design of molecular motor-based nanodevices for future bionanotechnology applications.

ACKNOWLEDGMENTS

This work was supported by DARPA (Grant No. N66001-02-C) and NSF (Grant No. BES 0428090). All experimental work was performed at the University of Michigan. We thank the staff members of the University of Michigan Lurie Nanofabrication Facility for their support in our fabrication of microtubule guiding assay sample chips.

[1] T. Kim, L. J. Cheng, M. T. Kao, E. F. Hasselbrink, L. J. Guo, and E. Meyhofer, Lab Chip **9**, 1282 (2009).
[2] M. G. L. van den Heuvel, M. P. De Graaff, and C. Dekker, Science **312**, 910 (2006).
[3] S. Ramachandran, K. H. Ernst, G. D. Bachand, V. Vogel, and H. Hess, Small **2**, 330 (2006).
[4] C. T. Lin, M. T. Kao, K. Kurabayashi, and E. Meyhofer, Nano Lett. **8**, 1041 (2008).
[5] J. L. Bull, A. J. Hunt, and E. Meyhofer, Biomed. Microdevices **7**, 21 (2005).
[6] C. T. Lin, M. T. Kao, K. Kurabayashi, and E. Meyhofer, Small **2**, 281 (2006).
[7] A. Goel and V. Vogel, Nat. Nanotechnol. **3**, 465 (2008).
[8] M. G. L. van den Heuvel and C. Dekker, Science **317**, 333 (2007).
[9] Y. Hiratsuka, T. Tada, K. Oiwa, T. Kanayama, and T. Q. P. Uyeda, Biophys. J. **81**, 1555 (2001).
[10] R. Yokokawa, S. Takeuchi, T. Kon, M. Nishiura, K. Sutoh, and H. Fujita, Nano Lett. **4**, 2265 (2004).
[11] T. Nitta, A. Tanahashi, M. Hirano, and H. Hess, Lab Chip **6**, 881 (2006).
[12] J. Clemmens, H. Hess, R. Lipscomb, Y. Hanein, K. F. Bohringer, C. M. Matzke, G. D. Bachand, B. C. Bunker, and V. Vogel, Langmuir **19**, 10967 (2003).
[13] F. Gittes, B. Mickey, J. Nettleton, and J. Howard, J. Cell Biol. **120**, 923 (1993).
[14] P. Venier, A. C. Maggs, M. F. Carlier, and D. Pantaloni, J. Biol. Chem. **269**, 13353 (1994).
[15] J. C. Kurz and R. C. Williams, Biochemistry **34**, 13374 (1995).
[16] C. Bouchiat, M. D. Wang, J. F. Allemand, T. Strick, S. M. Block, and V. Croquette, Biophys. J. **76**, 409 (1999).
[17] J. Howard, *Mechanics of Motor Proteins and the Cytoskeleton* (Sinauer Associates, Inc. Publishers, Sunderland, MA, 2001).
[18] A. J. Hunt and J. Howard, Proc. Natl. Acad. Sci. U.S.A. **90**, 11653 (1993).
[19] P. Katira, A. Agarwal, T. Fischer, H. Y. Chen, X. Jiang, J. Lahann, and H. Hess, Adv. Mater. **19**, 3171 (2007).
[20] M. Kurachi, M. Hoshi, and H. Tashiro, Cell Motil. Cytoskeleton **30**, 221 (1995).
[21] B. Mickey and J. Howard, J. Cell Biol. **130**, 909 (1995).
[22] T. Kim, M. T. Kao, E. F. Hasselbrink, and E. Meyhofer, Biophys. J. **94**, 3880 (2008).